Journal of Neuroimmunology 332 (2019) 147–154

Contents lists available at ScienceDirect

Journal of Neuroimmunology

journal homepage: www.elsevier.com/locate/jneuroim

IL-17A is associated with the breakdown of the blood-brain barrier in relapsing-remitting multiple sclerosis☆

A. Francesca Setiadi[a], Alexander R. Abbas[a], Surinder Jeet[a], Kit Wong[a], Antje Bischof[b,c], Ivan Peng[a], James Lee[a], Meire Bremer[a], Erica L. Eggers[b], Jason DeVoss[a,1], Tracy Staton[a], Ann Herman[a], H. -Christian von Büdingen[b,2], Michael J. Townsend[a,*]

[a] Genentech, Inc., 1 DNA Way, South San Francisco, CA 94080, USA
[b] Weill Institute for Neurosciences, Department of Neurology, UCSF, 675 Nelson Rising Lane, San Francisco, California 94158, USA
[c] Neurology and Neurologic Policlinic, Departments of Medicine, Biomedicine and Clinical Research, University Hospital Basel, Petersgraben 4, 4031 Basel, Switzerland

ABSTRACT

IL-17 has been implicated in the pathogenesis of multiple sclerosis (MS). Here, we show that blockade of IL-17A, but not IL-17F, attenuated experimental autoimmune encephalomyelitis (EAE). We further show that IL-17A levels were elevated in the CSF of relapsing-remitting MS (RRMS) patients and that they correlated with the CSF/serum albumin quotient (Qalb), a measure of blood-brain barrier (BBB) dysfunction. We then demonstrated that the combination of IL-17A and IL-6 reduced the expression of tight junction (TJ)-associated genes and disrupted monolayer integrity in the BBB cell line hCMEC/D3. However, unlike IL-17A, IL-6 in the CSF from RRMS patients did not correlate with Qalb. These data highlight the potential importance of targeting IL-17A in preserving BBB integrity in RRMS.

1. Introduction

Interleukin-17 (IL-17) is implicated in the pathogenesis of multiple sclerosis (MS). In active brain lesions, it is expressed by T helper 17 (Th17) cells and by astrocytes and oligodendrocytes in the central nervous system (CNS) where it synergizes with other pro-inflammatory cytokines and mediators of tissue damage (Kang et al., 2010; Tzartos et al., 2008; Waisman et al., 2015). IL-17A and IL-17F form homo- or heterodimers that bind to the IL-17 receptor complex (IL-17RA and IL-17RC) (Waisman et al., 2015). IL-17 disrupts barrier integrity of both human brain-derived primary microvascular endothelial cells (Kebir et al., 2007; Rahman et al., 2018) and a murine brain endothelial cell line, bEnd.3 (Huppert et al., 2010). IL-17 is important for the development of experimental autoimmune encephalomyelitis (EAE) (Langrish et al., 2005; McGinley et al., 2018). In IL-17A$^{-/-}$ mice, the blood-brain barrier (BBB) is less disrupted in induced EAE and disease scores are lower (Huppert et al., 2010). Pre-surgical treatment with anti-IL17A reduced BBB disruption in aged, wild-type C57BL/6 J mice that suffered from perioperative neurocognitive disorders (Ni et al., 2018).

Here, we applied a translational approach to study the effects of IL-17 on the development of experimental MS and BBB integrity. Blockade of IL-17A, but not IL-17F, attenuated disease activity in EAE. IL-17A was elevated in the CSF of RRMS patients, which was correlated with a

Abbreviations: BBB, blood-brain barrier; BCP, bromocresol purple; CNS, central nervous system; CFA, Complete Freund's Adjuvant; CSF, cerebrospinal fluid; dpi, day post-injection; EAE, experimental autoimmune encephalomyelitis; EDSS, Expanded Disability Status Scale; Gd, gadolinium; GFAP, glial fibrillary acidic protein; HD, healthy donors; IL-17, interleukin-17; i.p., intraperitoneal; LLOQ, lower limit of quantification; LY, lucifer yellow; Mab, monoclonal antibody; MEFs, mouse embryonic fibroblasts; MOG, myelin oligodendrocyte glycoprotein; MRI, magnetic resonance imaging; MS, multiple sclerosis; NFL, neurofilament light chain; OCB, oligoclonal band; PBS, phosphate buffer saline; Qalb, CSF/serum albumin quotient; qPCR, quantitative PCR; rh, recombinant human; rm., recombinant mouse; RRMS, relapsing-remitting multiple sclerosis; Rw, ragweed; TEER, trans-endothelial electrical resistance; Th17, T helper 17; TJ, tight junction; TNF-α, tumor necrosis factor-α

☆ This work was supported by Genentech, a member of the Roche Group. The funding source had no involvement in study design; in the collection, analysis and interpretation of data; in the writing of the report; and in the decision to submit the article for publication.

* Corresponding author.
E-mail address: townsem1@gene.com (M.J. Townsend).
[1] Current affiliation: Amgen, Inc., 1120 Veterans Blvd, South San Francisco, CA 94080, USA.
[2] Current affiliation: Roche Pharmaceutical Research and Early Development, Grenzacherstrasse 124, Basel 4070, Switzerland.

https://doi.org/10.1016/j.jneuroim.2019.04.011
Received 24 December 2018; Received in revised form 18 April 2019; Accepted 19 April 2019

surrogate measure of BBB integrity in 2 independent cohorts. Finally, a combination of IL-17A and IL-6 stimulation decreased *in-vitro* endothelial cell monolayer integrity.

2. Materials and methods

2.1. Antibody characterization

Anti-mouse IL-17A monoclonal antibody (Mab) (PRO97156) was produced in-house by transient co-expression of immunoglobulin sequences isolated from a single clonal hamster/mouse chimeric hybridoma along with mouse IgG2aκ DNA sequences in Chinese hamster ovary cells. Clonal hamster/mouse hybridoma lines were derived from hamsters immunized with mouse IL-17AA immunogen. Anti-mouse IL-17, anti-IL-17AF (clone 16H4.4F3, Novimmune, Switzerland) and anti-IL17F (clone 28E12, Novimmune, Switzerland) were confirmed to block recombinant IL-17A and F-induced mIL-6 by mouse embryonic fibroblasts (MEFs) derived from Il-17Rc-deficient mice reconstituted with FLAG-tagged IL-17RC as previously described (Hu et al., 2010).

MEFs were plated at 12.5×10^3 cells per well in a 96-well microtiter cell culture plate (Corning, Tewksbury, MA) in DMEM supplemented with 10% fetal bovine serum (Hyclone, Logan, UT), 2 mM GlutaMAX I (Invitrogen, Carlsbad, CA), 1 mM sodium pyruvate (Invitrogen), 0.1 mM non-essential amino acids (Hyclone), 55 μM 2-mercaptoethanol (Invitrogen), and 100 U/ml penicillin and 100 μg/ml streptomycin mixture (Invitrogen). After overnight incubation in a humidified incubator at 37 °C with 5% CO_2, cells were stimulated with the same medium containing 100 nM anti-IL-17 or an isotype matched control antibody as well as recombinant mouse (rm) IL-17AA, FF or AF protein (R&D Systems, Minneapolis, MN) at 1, 50 or 0.2 ng/ml, respectively. Each condition was carried out in triplicate. Supernatants were collected 2 days post-stimulation and the level of mIL-6 was measured using a mouse IL-6 DuoSet ELISA Kit (R&D Systems).

2.2. EAE development and anti-IL-17 antibodies treatment

The Institutional Animal Care and Use Committee (IACUC) at Genentech approved the protocols for animal experiments. All of the animal experiments were carried out in accordance with all applicable laws, regulations, guidelines, and policies governing the use of laboratory animals in research.

EAE was induced in 9-week-old female C57BL/6 mice. Mice were immunized subcutaneously with an emulsion containing myelin oligodendrocyte glycoprotein (MOG) 35–55 peptide (synthesized in-house) and Complete Freund's Adjuvant (CFA). Immunization was performed under isoflurane anesthesia. All animals received pertussis toxin (List Biological Laboratories, Campbell, CA) in PBS intraperitoneally (i.p.) on day 0 and day 2 after MOG immunization. Antibodies against IL-17 isoforms or control antibodies were used for the *in-vivo* treatment. Five groups of mice ($n = 8$ in the a-RW control group; $n = 10$ per group in the other groups) received antibodies 3 times per week by intraperitoneal (i.p.) injection (10 mg/kg per antibody), from day −1 to 30 post immunization (dpi). All mice were evaluated clinically 3 times per week from dpi 7 to 30; the person scoring the animals was blinded to the groups. The treatment groups included: anti-IL-17F, anti-IL17A, anti-IL-17AF, anti-IL-17AF + anti-IL17F, and anti-ragweed (Rw) control. At the end of the EAE experiment, animals were perfused with PBS following standard procedures, and spinal cords were harvested and snap-frozen for RNA extraction. All animal protocols were approved by the Genentech Inc. Institutional Animal Care and Use Committee.

2.3. RRMS patient samples and quantification of protein levels in the serum and CSF

Cohort 1: CSF from 50 RRMS patients and 20 HD (HD) were purchased from PrecisionMed, Inc., Solana Beach, CA; matching serum samples were obtained from all RRMS patients and 10 of the HD. No MRI data was available. Cohort 2: CSF and matching serum samples from 69 RRMS patients were obtained from the University of California, San Francisco (UCSF). The study was approved by the Ethics committee of the UCSF and adhered to the ethical principles for medical research involving human subjects of the Helsinki Declaration. Clinical MRI scans were collected using the UCSF picture archiving and communication system. MRI readings were performed blinded to the clinical and immunological data. Patient demographics and clinical characteristics are shown in Table 1.

Table 1
Demographic and clinical characteristics of RRMS patients and healthy donors (HD), NA not applicable, EDSS expanded disability status scale.

	HD cohort 1 ($n = 20$)	RRMS cohort 1 ($n = 50$)	RRMS cohort 2 ($n = 69$)
Age (yrs)			
Mean ± standard deviation (SD)	51 ± 5	51 ± 11	39 ± 11
Range	44–62	28–73	19–69
Gender			
Female	10 (50%)	38 (76%)	48 (70%)
Race & ethnicity			
Caucasian/Asian/Black/Hispanic/others or mixed	18 (90%)/0/1 (5%)/1 (5%)/0	45 (90%)/1 (2%)/2 (4%)/2 (4%)/0	59 (86%)/1 (1%)/5 (7%)/2 (3%)/2 (3%)
Disease duration			
Mean ± SD	na	12 ± 8 yrs	56 ± 133 days
Range	na	1–32 yrs	0–1017 days
Average EDSS (range)	na	4 (0–6.5)	2 (0–6)
Patients in MS medications			
Untreated/treated	na	15/35	52/17
Gd + presence in spine or brain			
+/−/unknown	na	na	28/13/28
T2-weighted lesions in spine or brain			
+/−/unknown	na	na	33/23/13
Oligoclonal bands			
+/−/unknown	na	na	55/10/4

Human IL-17A and IL-17F levels were quantified using the Singulex platform (Singulex, Alameda, CA) as previously described (Schofield et al., 2016). Pro-inflammatory cytokines and chemokines were quantified using a combination of electrochemiluminescence and multi-array technology (McKay et al., 2017). ELISA-based assays were performed to measure the levels of neurofilament light chain (NFL) (UmanDiagnostics, Umea, Sweden) and glial fibrillary acidic protein (GFAP) (BioVendor Inc., Asheville, NC). Albumin in "Cohort 1" was measured using Human Serum Albumin ELISA kit (Sigma-Aldrich, St. Louis, MO). In "Cohort 2", albumin was measured in the UCSF clinical laboratory using bromocresol purple (BCP) reagent and at Quest Diagnostics (various locations, USA) using Fixed Rate Time Nephelometry; the albumin quotient (Qalb) was calculated as the ratio of CSF/serum albumin. Concentration of analytes that fell below the lower limit of quantification (LLOQ) were imputed as half of the LLOQ of the assay. Quantification of all proteins was performed prior to freeze-thaw cycles.

2.4. Human brain endothelial cell culture, cytokine treatments and RNA extraction

Human cerebral microvascular endothelial cells (hCMEC/D3) (Weksler et al., 2013; Weksler et al., 2005) at passages 26–35 were cultured on rat-tail collagen type I-coated tissue culture plates (for gene expression studies) or Transwell® inserts (for assessments of cell monolayer integrity) containing EBM-2 basal medium (Lonza, Walkersville, MD) supplemented with the EGM-2 SingleQuot reagents

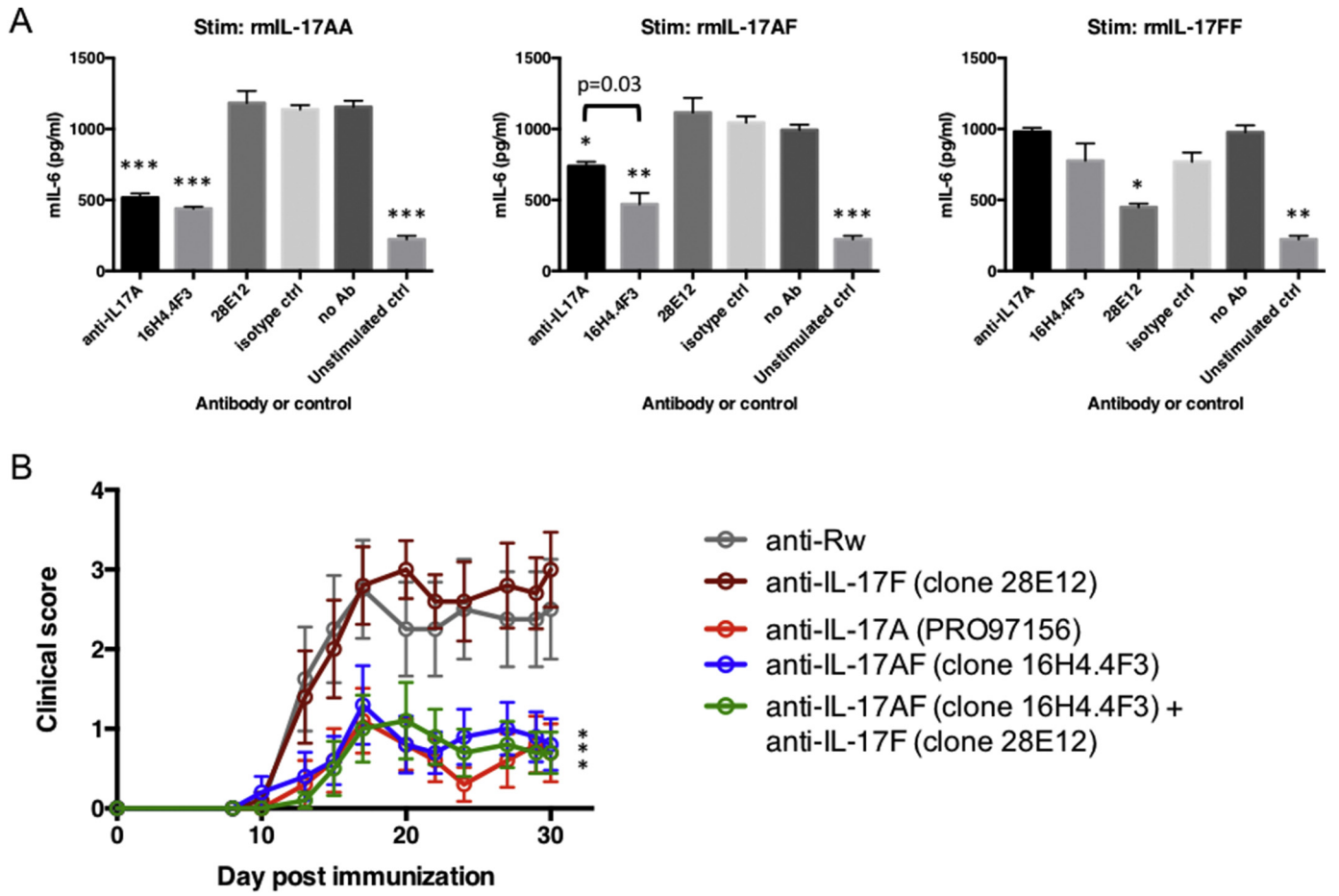

Fig. 1. Blockade of specific IL-17 subsets by anti-mouse IL-17 antibodies and attenuation of EAE development. (A) mIL-6 production by rmIL-17AA and IL-17AF-stimulated MEFs was reduced upon treatment with the antibody clone 16H4.4F3, while clone 28E12 only blocked the mIL-6 production upon stimulation of MEFs with rmIL-17FF. Columns: mean of triplicates; error bars: SEM; $*p < .05$, $**p < .0004$, $***p < .0001$ *vs.* isotype and no Ab controls by ANOVA with Dunnett's test. Data is representative of five independent experiments. (B) *In-vivo* blockades of IL-17A and IL-17AF were efficacious in attenuating EAE development. Clinical scores were significantly lower in the group treated with anti-IL-17A (PRO97156), anti-IL-17AF (clone 16H4.4F3) or a combination of anti-IL-17AF + anti-IL-17F (clone 16H4.4F3 + 28E12) compared to anti-Rw control ($*p < .03$ for average clinical scores on day 30 comparisons for each group with the anti-Rw control by ANOVA with Dunnett's test). $n = 10$ mice per treatment group except $n = 8$ in the anti-RW control group; plots: mean; error bars: SEM.

obtained from the manufacturer. Cells were maintained at 37 °C and 5% CO2 until confluence. Immortalized hCMEC/D3 cell line was kindly provided by Ashley Hayes, F. Hoffmann-La Roche Ltd., Basel, Switzerland. Rat-tail collagen type I was obtained from Gibco, Madison, WI.

Recombinant human (rh) IL17A, rhTNF-α, rhIL6 and rhIL6R were purchased from R&D Systems. The experiments were run in 2-fold serial dilutions for each cytokine. Final concentrations used in this study: 50 ng/ml IL-17A ± 1 ng/ml TNF-α or 25 ng/ml IL-6 + 50 ng/ml IL-6R. For gene expression analyses, total RNA was extracted using RNeasy Mini Kit (QIAGEN) after 2 days of treatment with the cytokines.

2.5. Quantitative real-time PCR (qPCR)

Complementary DNA (cDNA) was synthesized using iScript cDNA Synthesis Kit (Biorad, Hercules, CA) using 100 ng RNA per sample. Following pre-amplification steps, gene expression changes were assessed using Fluidigm® 96.96 Dynamic Array, according to the manufacturer's protocol (Fluidigm, South San Francisco, CA). All gene expression results are expressed as arbitrary units relative to the geometric mean of human glyceraldehyde 3-phosphate dehydrogenase (Gapdh), hypoxanthine-guanine phosphoribosyl transferase (Hprt1) and beta-glucuronidase (Gusb) as normalizing genes. TaqMan probes were purchased from Thermo Fisher Scientific (Waltham, MA). Probe IDs are as follows: *Ocln*: Hs00170162_m1, *Tjp1*: Hs01551861_m1, *Cdh5*: Hs00901465_m1, *Pecam1*: Hs01065282_m1, *Jam1*: Hs00170991_m1, *Cldn3*: Hs00265816_s1, *Cldn5*: Hs00533949_s1, *Gapdh*: Hs99999905_m1, *Hprt1*: Hs01003267_m1, *Gusb*: Hs00939627_m1.

2.6. Assessment of cell monolayer integrity by trans-endothelial electrical resistance (TEER) measurement and lucifer yellow (LY) fluorescent marker

hCMEC/D3 cells were seeded at 6.0×10^4 cells/cm^2 on the apical side of an 0.4 μm polyester membrane (Corning, NY) pre-coated with rat-tail collagen type I. The cells were grown on the 6.5 mm-diameter, 24-well tissue culture Transwell® inserts for 4 days to near confluency, prior to an exchange of medium and 1 to 3 days of treatment with the cytokines. The monolayer integrity was assessed by (TEER) measurement (Srinivasan et al., 2015). Cells cultured on the inserts were allowed to equilibrate to room temperature for 20 min. A small aliquot of cells from each treatment group was set aside and stained with trypan blue (Life Technologies, Carlsbad, CA) to confirm > 95% viability. An EVOM™ Epithelial Voltohmmeter and chopstick electrodes (World Precision Instruments, UK) were used for the measurement of the electrical resistance of endothelial cell monolayers. Monolayer TEER values, reported in units of Ω (ohms).cm^2, was calculated by subtracting the resistance (ohm) of a collagen I-coated insert without cells from the readings obtained on a coated insert with cells, and multiplied by the surface area of the insert (0.33 cm^2). Results are expressed as

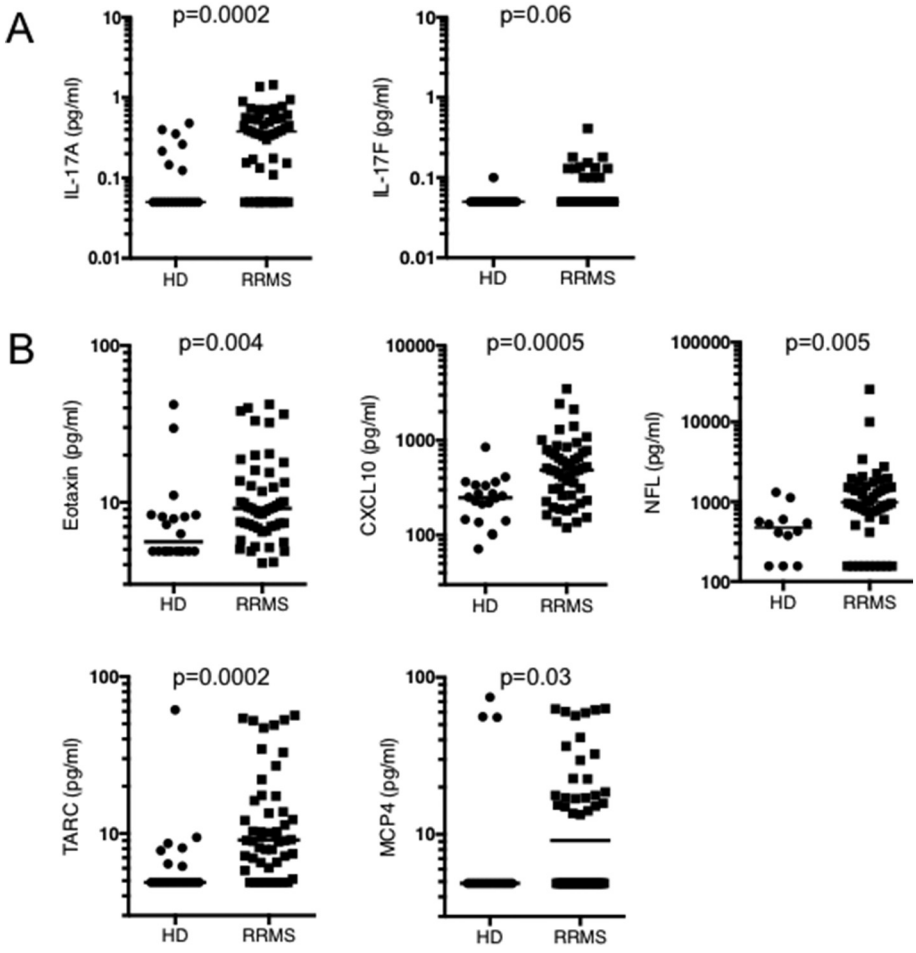

Fig. 2. Assessment of IL-17 and pro-inflammatory chemokines levels in the CSF from Cohort 1 RRMS patients ($n = 50$) and HD ($n = 20$). (A) IL-17A was elevated in the CSF from RRMS patients *vs.* HD ($p = .0002$ by Wilcoxon rank sum test). IL-17F was elevated in the CSF from some RRMS patients; however, the difference *vs.* HD was not significant ($p = .06$ by Wilcoxon rank sum test). Lines: median. (B) NFL and pro-inflammatory chemokines were elevated in the CSF from RRMS patients *vs.* HD ($p < .04$ by Wilcoxon rank sum test). Lines: median.

means ± standard error of the mean (SEM). $N = 11$ wells per treatment or PBS control.

Paracellular permeabilities of LY ((Eigenmann et al., 2013) were also determined after 3 days of cytokines treatment, where tissue culture inserts were transferred into a 24-well plate containing 500 µL of pre-warmed (37 °C) Ringer HEPES buffer (150 mM NaCl, 2.2 mM CaCl2, 0.2 mM MgCl2, 5.2 mM KCl, 2.8 mM glucose, 5 mM HEPES, and 6 mM NaHCO3, pH 7.4) per well (basolateral compartment). Medium in inserts (apical compartment) was then replaced with 200 µL of a pre-warmed (37 °C) working solution containing LY at 100 µM in Ringer HEPES buffer. The 24-well plate was incubated with shaking at 37 °C and basolateral supernatants were quantified for fluorescence (excitation 485 nm, emission 528 nm) using a Synergy 2 microplate reader (BioTek, Winooski, VT) using the calculation % permeability = ((fluorescence with cells - blank)/(fluorescence without cells - blank)) x 100%. Percent permeability of a collagen I-coated control insert without cells was assigned a value of 100%. Results were expressed as means ± SEM. $N = 11$ wells per treatment or PBS control.

2.7. Statistical analyses

All statistical comparisons were made using either a Wilcoxon rank sum test on each pair (unadjusted for multiple hypothesis testing) or ANOVA with Dunnett's test. For all tests, $p < .05$ was considered significant and $0.05 \leq p \leq .1$ was considered a trend. Correlation analyses were done using Spearman's method.

3. Results

3.1. Blockade of IL-17A, but not IL-17F, attenuated the development of EAE

Cell-based assays showed that the anti-IL-17A Mab (PRO97156) and anti-IL17-AF (16H4.4F3) blocked both IL-17AA and IL-17AF (Fig. 1A). The IL-17AF blockade was more pronounced by anti-IL-17AF than by anti-IL-17A ($p = .03$ by ANOVA with Dunnett's test). Anti-IL-17F (28E12) significantly blocked the stimulatory effect of rmIL-17FF.

In EAE, preventative anti-IL-17 treatment lowered clinical scores compared to anti-Rw controls in groups treated with anti-IL-17A or any antibody combination that included anti-IL17A: anti-IL-17AF (clone 16H4.4F3) and anti-IL-17AF + anti-IL-17F (clone 16H4.4F3 + 28E12). Anti-IL-17F alone did not lower the clinical scores (Fig. 1B).

3.2. Elevated IL-17A in the CSF from RRMS patients correlated with Qalb in cohort 1

Levels of IL-17A and F in the CSF from RRMS patients and healthy donors (HD) were assessed with an immunoassay that resolved IL-17A and IL-17F isoforms (Schofield et al., 2016). IL-17A was detectable in the CSF in 38/50 (76%) RRMS patients and in 7/20 (35%) HD. It was elevated in the CSF from RRMS patients ($n = 50$) *vs.* HD ($n = 20$) (Fig. 2A). IL-17F was also detectable in the CSF from 12/50 (24%) RRMS patients and 1/20 (5%) HD; however, the levels in RRMS *vs.* HD were not significantly different (Fig. 2A).

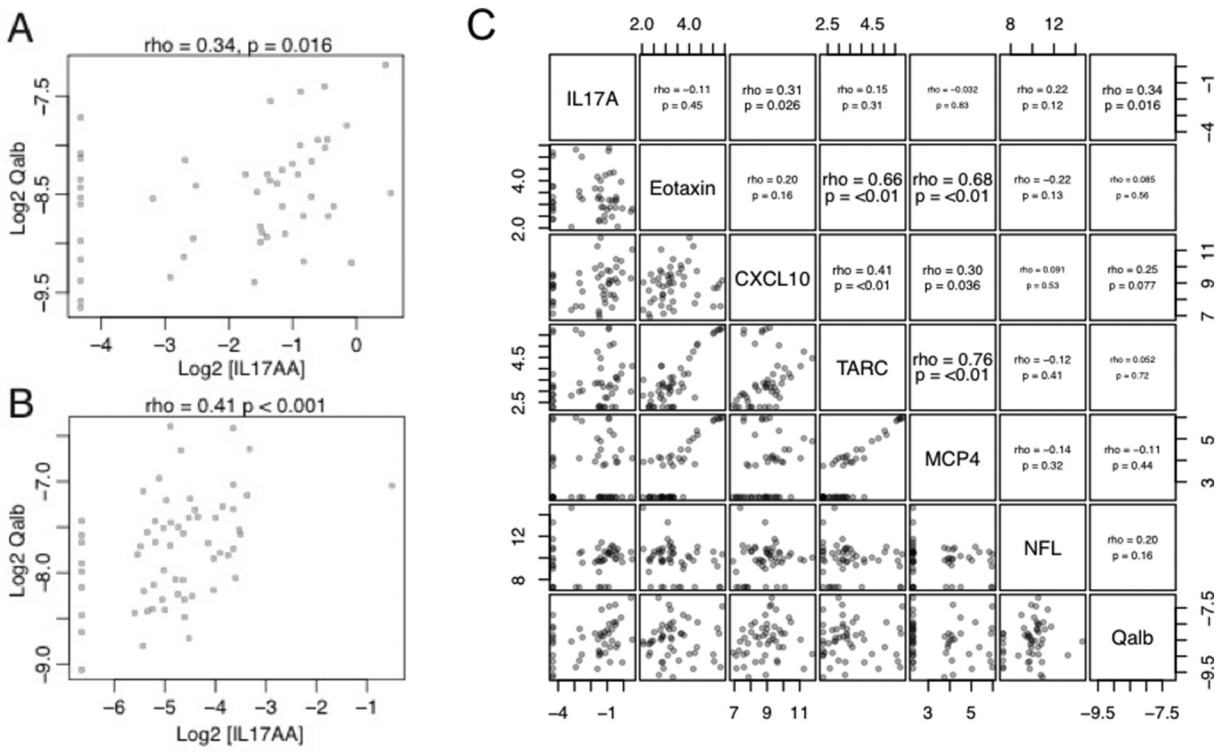

Fig. 3. Correlation analyses of IL-17A, NFL and pro-inflammatory chemokines in the RRMS CSF and Qalb. IL-17A correlated with Qalb in RRMS (A) Cohort 1 and (B) Cohort 2. (C) NFL and chemokines that were found to be elevated in the RRMS CSF *vs.* HD in Cohort 1 did not correlate with the Qalb.

Since IL-17A has previously been reported to play important roles in CNS inflammatory responses (Waisman et al., 2015), we measured inflammatory proteins, chemokines and cytokines in the CSF as well as the CSF levels of markers of neuronal (NFL) and glial cell damage (GFAP) (Constantinescu et al., 2016). Eotaxin, CXCL10, TARC, MCP4, and NFL were significantly higher in the RRMS CSF *vs.* HD (Fig. 2B). Elevated levels of CRP, SAA, ICAM1, VCAM1 and cytokines such as IFN-γ, IL-8, IL-12, IL-1β, IL-2, IL-6 and TNF-α were observed in the CSF from some RRMS patients; however, the differences *vs.* HD were not statistically significant ($p > .05$, Wilcoxon rank sum test). GFAP was not elevated in RRMS CSF *vs.* HD ($p = .8$, Wilcoxon rank sum test).

We determined whether the levels of IL-17A in the CSF were associated with the Qalb, a measure of patients' impairment of BBB integrity (Anckarsater et al., 2005; Reiber, 2001; Tibbling et al., 1977), age, gender, disease duration or Expanded Disability Status Scale (EDSS). We found a positive correlation between IL-17A and Qalb (Spearman's rho = 0.34; $p = .016$) (Fig. 3A). Although NFL, Eotaxin, CXCL10, TARC and MCP4 were significantly elevated in the RRMS CSF, these did not correlate with Qalb (Fig. 3C), suggesting a direct contribution of IL-17A to BBB damage. Male patients displayed higher levels of CSF IL-17A than female patients (Supplementary Fig. 1A, $p = .001$). No other correlation was observed between CSF IL-17A and other patients' demographics and clinical parameters, including MS medication status (Supplementary Fig. 2A, $p = .9$).

3.3. Correlation of IL-17A in CSF with Qalb in a second, independent cohort of RRMS patients with < 1 year of disease

We assessed a second RRMS cohort ($n = 69$) with MRI data available (Table 1). This cohort contained an earlier stage of RRMS with lower EDSS scores than the first cohort (Table 1). The levels of CSF IL-17A and pro-inflammatory chemokines (MCP1, MIP-1b and TARC) were lower than the first cohort, although CXCL10 levels were similar (Supplementary Fig. 3).

Despite these differences, we found that, similar to the first cohort, CSF IL-17A levels also correlated with Qalb in this second cohort (Fig. 3B). No significant relationships between CSF IL-17A levels and the presence of oligoclonal bands (OCB), cervical and thoracic T2 lesions in the spine, and Gadolinium (Gd+) T1 lesions in the spine and brain were observed (Supplementary Table 1). Further, no correlation was observed between the number of T1 Gd + lesions in spine and brain with CSF IL-17A levels (Spearman's rho was 0.1 ($p = .5$) and − 0.03 ($p = .8$), respectively) as reported in Supplementary Table 2.

Unlike the first cohort, no gender difference in CSF IL-17A levels were observed in the second cohort (Supplementary Fig. 1B, $p = .4$), but a weak, inverse correlation was observed between CSF IL-17A and age (Supplementary Table 2, Spearman's rho = −0.2, $p = .04$). No other correlation was observed between CSF IL-17A and MS medication status (Supplementary Fig. 2B, $p = .7$), MRI findings, disease duration and EDSS (Supplementary Table 2).

3.4. Treatment of endothelial cells with rhIL-17A in the presence of IL-6 + IL-6R reduced tight junction gene expression and impaired endothelial cell monolayer integrity

We treated the hCMEC/D3 brain endothelial cell line with rhIL-17A for 2 days, in the presence of TNF-α or IL-6 + IL-6R that had been implicated in MS pathogenesis and BBB breakdown (Jadidi-Niaragh and Mirshafiey, 2011; Luchtman et al., 2014; Minagar and Alexander, 2003; Montgomery and Bowers, 2012; Quintana et al., 2009), to assess the response of genes encoding TJ-associated proteins (*Ocln*, *Tjp1*, *Jam1*, *Cldn3* and *Cldn5*), an adherens junction protein and adhesion molecule, *Cdh5* and *Pecam1*, respectively, that are known to be expressed in the cell line (Weksler et al., 2005). The expression of 4 genes (*Ocln*, *Tjp1*, *Cdh5* and *Pecam1*) was significantly reduced after IL-17A + IL-6 + IL-6R treatment, compared to PBS control. *Jam1* trended down after IL-17A + IL-6 + IL-6R treatment. Significant *Pecam1* decrease and a trend for *Cdh5* and *Tjp1* decrease were observed upon treatment of the cells with IL-17A alone. The most pronounced

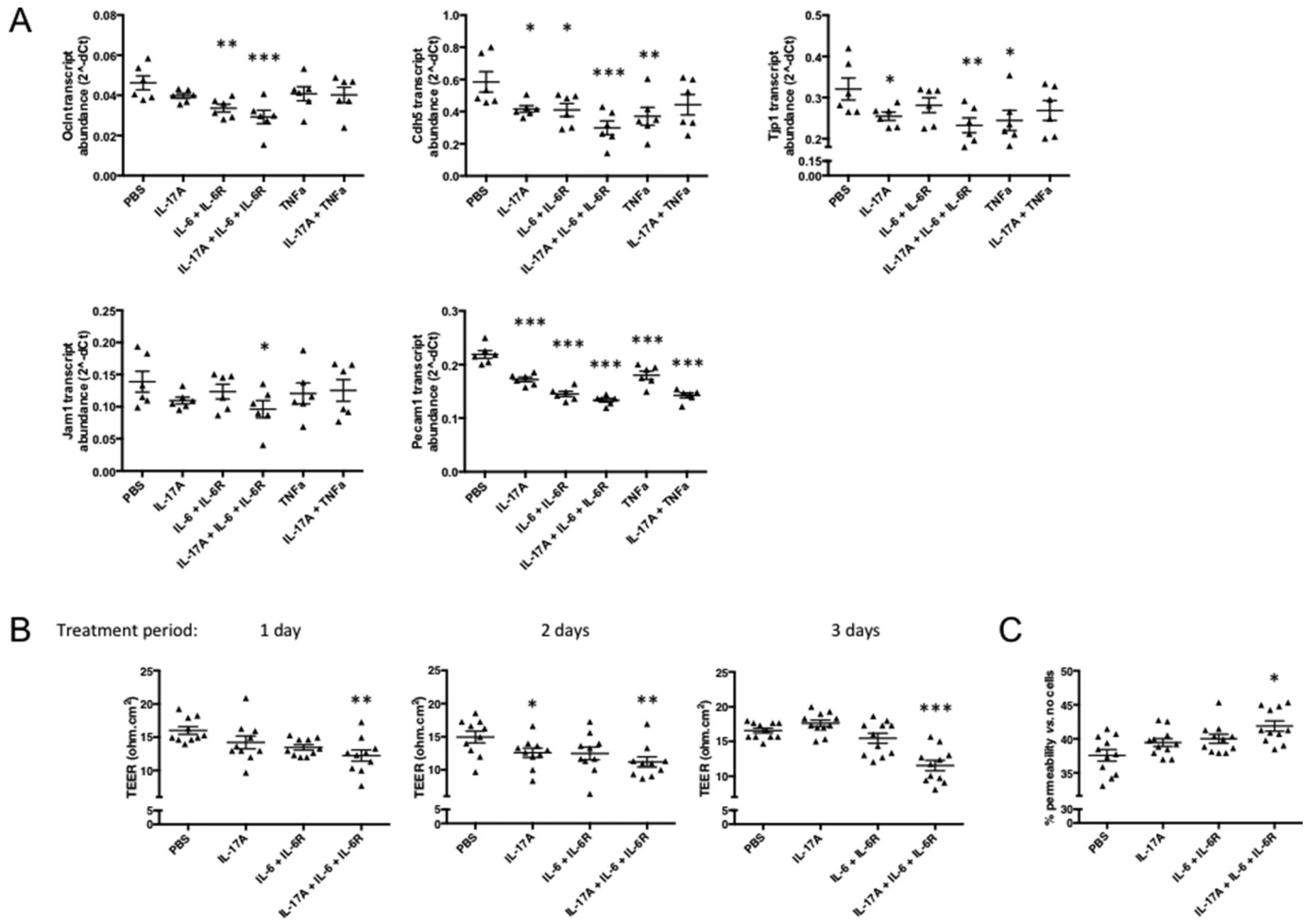

Fig. 4. Decreased expression of genes encoding for cellular and tight junction-associated proteins and a reduction of the cell monolayer integrity upon treatment of hCMEC/D3 cells with IL-17A + IL-6 + IL-6R. Data is representative of three independent experiments. (A) Decreased expression of Ocln, Tjp1, Cdh5, Pecam1 and Jam1 (*$p = .1$, **$p < .03$, ***$p < .003$) *vs.* PBS control by ANOVA with Dunnett's test). Treatment period: 2 days; $n = 6$ per group; plots: mean; error bars: SEM. (B) Decrease of TEER (*$p = .1$, **$p < .009$, ***$p < .0001$ *vs.* PBS control by ANOVA with Dunnett's test). Treatment period: 1–3 days; $n = 10$–11 per group; plots: mean; error bars: SEM. (C) Increase in monolayer permeability (*$p = .0004$ *vs.* PBS control by ANOVA with Dunnett's test). Treatment period: 3 days; $n = 11$ per group; plots: mean; error bars: SEM.

reduction in the expression of the 5 genes occurred with a combination of IL-17A and IL-6 + IL-6R. Expression of *Pecam1* and *Cdh5* was also significantly decreased with TNF-α alone, and *Pecam1* was further reduced with a combination of IL-17A and TNF-α (Fig. 4A). *Cldn3* and *Cldn5* expression levels were not affected by any of the treatments (data not shown).

We then assessed monolayer integrity after treatment with IL-17A ± IL-6 + IL-6R using TEER and solute transport assays. IL17A alone did not significantly decrease the TEER (Fig. 4B) or increase permeability of the cell monolayer to LY (Fig. 4C). In contrast, IL-17A + IL-6 + IL-6R lowered the TEER compared to PBS control as soon as 1 day after treatment (Fig. 4B). The monolayer in the IL-17A + IL-6 + IL-6R treated group also displayed higher permeability to LY *versus* PBS control as assessed after 3 days of treatment (Fig. 4C).

4. Discussion

We found that IL-17A, but not IL-17F, contributed to EAE pathogenesis. This observation is consistent with previous reports that CNS-infiltrating Th17 cells in EAE predominantly expressed IL-17A, and the expression of IL-17F was associated with non-pathogenic Th17 cells (Wanke et al., 2018).

Analyses of IL-17A levels in the CSF from two independent cohorts of RRMS patients showed a consistent result that CSF IL-17A positively correlated with Qalb, a measure of BBB damage in RRMS. This is the first report that CSF IL-17A levels were positively correlated with Qalb in RRMS, in both the early (Cohort 2) and late (Cohort 1) stages of the disease. The positive correlation in the early RRMS cohort suggests that IL-17A could play a role in early BBB disruption during MS pathophysiology. A direct contribution of IL-17A to BBB damage was further supported by the observation that other pro-inflammatory chemokines that were significantly elevated in the Cohort 1 RRMS CSF, such as Eotaxin, CXCL10, TARC and MCP4, did not correlate with the Qalb.

In the RRMS Cohort 2, we found a lack of correlation between CSF IL-17A levels and the presence OCB, as well as with the numbers of T1 Gd + and T2 lesions. A previous study reported that the number and the volume of Gd-enhancing lesions are highly correlated (Rovaris et al., 1999). Although the presence of Gd + lesions in the CNS indicates active lesions, it may underrepresent the overall extent of BBB disruption (Waubant, 2006). The lack of correlation between IL-17A levels and Gd positivity suggests that IL-17A elevation is not solely explained by the presence of active lesions. Although relapse information was not collected for the cohorts studied, and the absence of correlation with EDSS and MRI Gd^+ lesions suggests that there is also no correlation with relapse activity. To further address whether medication treatment may have confounded these results (for example,

treatment escalation may have occurred due to ongoing disease activity and/or may have affected CSF IL-17A levels), we analyzed the levels of CSF IL-17A in patients who were treated *vs.* untreated. The results indicated similar levels of CSF IL-17A in treated *vs.* untreated patients in both RRMS cohorts (Supplementary Fig. 2).

The presence of IL-6 signaling alongside IL-17A was shown to be important on disrupting barrier function in hCMEC/D3 human brain endothelial cell line, by decreasing the expression of genes encoding tight junction, adherens junction and adhesion proteins. IL-17A has also been reported to disrupt the BBB through modification of the localization of TJ proteins and the underlying cytoskeleton (Rahman et al., 2018). Therefore, multiple levels of regulation of this process by IL-17A are possible. IL-17 by itself has been reported to have the ability to disrupt the barrier integrity of human brain-derived primary microvascular endothelial cells (Kebir et al., 2007) and a murine brain endothelial cell line, bEnd.3, at a higher concentration (Huppert et al., 2010). However, in our system, the effects of IL-17A alone are not sufficient to result in the disruption of the barrier integrity of the hCMEC/D3 cell line. We believe this difference in response to IL-17A could be attributed to different sensitivity of different cells to IL-17A. Synergistic effect of IL-6 and IL-17 has been shown in previous studies using other cell types, such as astrocytes (Ma et al., 2010) and structural lung cells (van den Berg et al., 2005). This also appears to be the case in our system, where the stronger effect of combining of IL-6 and IL-17A is required to see physiological effects on the brain endothelial cells monolayer permeability.

Our studies of EAE mice and human CSF showed the importance of IL-17A, but not IL-17F, in EAE development and in RRMS in humans where its elevation in CSF was accompanied by increased BBB permeability. These data support a previous report that IL-17A ablation reduced BBB disruption in EAE (Huppert et al., 2010). Experiments using the human brain endothelial cell line hCMEC/D3 indicated that a combination of IL-17A and IL-6 impaired monolayer integrity and increased paracellular permeability. However, unlike IL-17A, IL-6 in the RRMS CSF did not correlate with the BBB damage marker or with the IL-17A itself, as assessed in Cohort 1 (Spearman's rho = -0.01 ($p = .9$) and -0.2 ($p = .2$), respectively). Taken together, our findings reaffirm the importance of IL-17A, likely acting as an amplifier of inflammatory cytokine signaling, as a mediator of tissue damage in RRMS and should be considered as a therapeutic target to preserve BBB integrity in these patients, potentially in combination with other inflammatory cytokines such as IL-6.

Supplementary data to this article can be found online at https://doi.org/10.1016/j.jneuroim.2019.04.011.

Author contributions

A. Francesca Setiadi and Michael J. Townsend conceived the work and designed the study. A. Francesca Setiadi, Surinder Jeet, Kit Wong, Ivan Peng, James Lee, Erica Eggers, Antje Bischof and Meire Bremer performed experiments and collected the data. A. Francesca Setiadi, Alexander R. Abbas, Surinder Jeet, Kit Wong and Ivan Peng analyzed the data. A. Francesca Setiadi, Alexander R. Abbas and Kit Wong wrote the manuscript and provided Figures. Tracy Staton, Jason DeVoss, Ann Herman, H.-Christian von Büdingen, Michael J. Townsend critically reviewed the manuscript and gave final approval for submission.

Competing interests

AFS, ARA, SJ, KW, IP JL, MB, TS, AH and MJT are employees of Genentech, Inc., a member of the Roche Group. JD was an employee of Genentech during the preparation of this manuscript. HCB is currently an employee of Roche. The other authors do not have any financial conflicts of interest.

Acknowledgements

We thank Eugene Chen and Emile Plise for contributing reagents and scientific discussions; Neko Ota, Kurt Schroeder, Leonard Dragone, Marcel van der Brug, Wenjun Ouyang and Tracy Yuen for scientific discussions; Oleg Mayba and Bill Forrest for statistical analyses consultation; Sarah Jahn, Mia Derstine, Max Kazer, Aya Abounasr, Natalie Pierson and William Harkin for assistance with CSF collection and clinical data organization at the University of California, San Francisco, CA. These studies were supported by Genentech, a member of the Roche Group.

References

Anckarsater, H., Forsman, A., Blennow, K., 2005. Increased CSF/serum albumin ratio: a recurrent finding in violent offenders. Acta Neurol. Scand. 112, 48–50.
Constantinescu, R., Krysl, D., Bergquist, F., Andren, K., Malmestrom, C., Asztely, F., et al., 2016. Cerebrospinal fluid markers of neuronal and glial cell damage to monitor disease activity and predict long-term outcome in patients with autoimmune encephalitis. Eur. J. Neurol. 23, 796–806.
Eigenmann, D.E., Xue, G., Kim, K.S., Moses, A.V., Hamburger, M., Oufir, M., 2013. Comparative study of four immortalized human brain capillary endothelial cell lines, hCMEC/D3, hBMEC, TY10, and BB19, and optimization of culture conditions, for an in vitro blood-brain barrier model for drug permeability studies. Fluids Barriers CNS. 10, 33.
Hu, Y., Ota, N., Peng, I., Refino, C.J., Danilenko, D.M., Caplazi, P., et al., 2010. IL-17RC is required for IL-17A- and IL-17F-dependent signaling and the pathogenesis of experimental autoimmune encephalomyelitis. J. Immunol. 184, 4307–4316.
Huppert, J., Closhen, D., Croxford, A., White, R., Kulig, P., Pietrowski, E., et al., 2010. Cellular mechanisms of IL-17-induced blood-brain barrier disruption. FASEB J. 24, 1023–1034.
Jadidi-Niaragh, F., Mirshafiey, A., 2011. Th17 cell, the new player of neuroinflammatory process in multiple sclerosis. Scand. J. Immunol. 74, 1–13.
Kang, Z., Altuntas, C.Z., Gulen, M.F., Liu, C., Giltiay, N., Qin, H., et al., 2010. Astrocyte-restricted ablation of interleukin-17-induced Act1-mediated signaling ameliorates autoimmune encephalomyelitis. Immunity. 32, 414–425.
Kebir, H., Kreymborg, K., Ifergan, I., Dodelet-Devillers, A., Cayrol, R., Bernard, M., et al., 2007. Human TH17 lymphocytes promote blood-brain barrier disruption and central nervous system inflammation. Nat. Med. 13, 1173–1175.
Langrish, C.L., Chen, Y., Blumenschein, W.M., Mattson, J., Basham, B., Sedgwick, J.D., et al., 2005. IL-23 drives a pathogenic T cell population that induces autoimmune inflammation. J. Exp. Med. 201, 233–240.
Luchtman, D.W., Ellwardt, E., Larochelle, C., Zipp, F., 2014. IL-17 and related cytokines involved in the pathology and immunotherapy of multiple sclerosis: current and future developments. Cytokine Growth Factor Rev. 25, 403–413.
Ma, X., Reynolds, S.L., Baker, B.J., Li, X., Benveniste, E.N., Qin, H., 2010. IL-17 enhancement of the IL-6 signaling cascade in astrocytes. J. Immunol. 184, 4898–4906.
McGinley, A.M., Edwards, S.C., Raverdeau, M., Mills, K.H.G., 2018. Th17cells, gamma-delta T cells and their interplay in EAE and multiple sclerosis. J. Autoimmun. 87, 97–108.
McKay, H.S., Margolick, J.B., Martinez-Maza, O., Lopez, J., Phair, J., Rappocciolo, G., et al., 2017. Multiplex assay reliability and long-term intra-individual variation of serologic inflammatory biomarkers. Cytokine. 90, 185–192.
Minagar, A., Alexander, J.S., 2003. Blood-brain barrier disruption in multiple sclerosis. Mult. Scler. 9, 540–549.
Montgomery, S.L., Bowers, W.J., 2012. Tumor necrosis factor-alpha and the roles it plays in homeostatic and degenerative processes within the central nervous system. J. NeuroImmune Pharmacol. 7, 42–59.
Ni, P., Dong, H., Wang, Y., Zhou, Q., Xu, M., Qian, Y., et al., 2018. IL-17A contributes to perioperative neurocognitive disorders through blood-brain barrier disruption in aged mice. J. Neuroinflammation 15, 332.
Quintana, A., Muller, M., Frausto, R.F., Ramos, R., Getts, D.R., Sanz, E., et al., 2009. Site-specific production of IL-6 in the central nervous system retargets and enhances the inflammatory response in experimental autoimmune encephalomyelitis. J. Immunol. 183, 2079–2088.
Rahman, M.T., Ghosh, C., Hossain, M., Linfield, D., Rezaee, F., Janigro, D., et al., 2018. IFN-gamma, IL-17A, or zonulin rapidly increase the permeability of the blood-brain and small intestinal epithelial barriers: relevance for neuro-inflammatory diseases. Biochem. Biophys. Res. Commun. 507, 274–279.
Reiber, H., 2001. Dynamics of brain-derived proteins in cerebrospinal fluid. Clin. Chim. Acta 310, 173–186.
Rovaris, M., Bastianello, S., Capra, R., Comi, G., Yousry, T.A., Filippi, M., 1999. Correlation between enhancing lesion number and volume on standard and triple dose gadolinium-enhanced brain MRI scans from patients with multiple sclerosis. Magn. Reson. Imaging 17, 985–988.
Schofield, C., Fischer, S.K., Townsend, M.J., Mosesova, S., Peng, K., Setiadi, A.F., et al., 2016. Characterization of IL-17AA and IL-17FF in rheumatoid arthritis and multiple sclerosis. Bioanalysis. 8, 2317–2327.
Srinivasan, B., Kolli, A.R., Esch, M.B., Abaci, H.E., Shuler, M.L., Hickman, J.J., 2015. TEER measurement techniques for in vitro barrier model systems. J. Lab. Autom. 20, 107–126.

Tibbling, G., Link, H., Ohman, S., 1977. Principles of albumin and IgG analyses in neurological disorders. I. Establishment of reference values. Scand. J. Clin. Lab. Invest. 37, 385–390.
Tzartos, J.S., Friese, M.A., Craner, M.J., Palace, J., Newcombe, J., Esiri, M.M., et al., 2008. Interleukin-17 production in central nervous system-infiltrating T cells and glial cells is associated with active disease in multiple sclerosis. Am. J. Pathol. 172, 146–155.
van den Berg, A., Kuiper, M., Snoek, M., Timens, W., Postma, D.S., Jansen, H.M., et al., 2005. Interleukin-17 induces hyperresponsive interleukin-8 and interleukin-6 production to tumor necrosis factor-alpha in structural lung cells. Am. J. Respir. Cell Mol. Biol. 33, 97–104.
Waisman, A., Hauptmann, J., Regen, T., 2015. The role of IL-17 in CNS diseases. Acta Neuropathol. 129, 625–637.
Wanke, F., Tang, Y., Gronke, K., Klebow, S., Moos, S., Hauptmann, J., et al., 2018. Expression of IL-17F is associated with non-pathogenic Th17 cells. J. Mol. Med. (Berl). 96, 819–829.
Waubant, E., 2006. Biomarkers indicative of blood-brain barrier disruption in multiple sclerosis. Dis. Markers 22, 235–244.
Weksler, B.B., Subileau, E.A., Perriere, N., Charneau, P., Holloway, K., Leveque, M., et al., 2005. Blood-brain barrier-specific properties of a human adult brain endothelial cell line. FASEB J. 19, 1872–1874.
Weksler, B., Romero, I.A., Couraud, P.O., 2013. The hCMEC/D3 cell line as a model of the human blood brain barrier. Fluids Barriers CNS. 10, 16.